Identification of flutter derivatives of bridge decks using CFD-based discrete-time aerodynamic models

Zhiwen Zhu[1a] and Ming Gu[*2]

[1]*Center of Wind Engineering, Hunan University, Changsha 410082, China*
[2]*State Key Laboratory for Disaster Reduction in Civil Engineering, Tongji University, Shanghai 200092, China*

Abstract. This paper presents a method to extract flutter derivatives of bridge decks based on a combination of the computational fluid dynamics (CFD), system simulations and system identifications. The incompressible solver adopts an Arbitrary Lagrangian-Eulerian (ALE) formulation with the finite volume discretization in space. The imposed sectional motion in heaving or pitching relies on exponential time series as input, with aerodynamic forces time histories acting on the section evaluated as output. System identifications are carried out to fit coefficients of the inputs and outputs of ARMA models, as to establish discrete-time aerodynamic models. System simulations of the established models are then performed as to obtain the lift and moment exerting on the sections to a sinusoidal displacement. It follows that flutter derivatives are identified. The present approaches are applied to a hexagon thin plate and a real bridge deck. The results are compared to the Theodorsen closed-form solution and those from wind tunnel tests. Satisfactory agreements are observed.

Keywords: bridge flutter; CFD; discrete-time aerodynamic model; system identification; system simulation

1. Introduction

Wind effects are of great importance in design and construction of long-span bridges due to their slenderness and flexibility. The dynamic stability of super-long span bridges at high wind speeds often governs the structural design due to the potentially catastrophic nature of flutter instability. When dealing with the flutter instability, the self-excited forces arising from the motion of the bridge deck in airflow can be treated as a linear combination of displacements, velocities and flutter derivatives (Scanlan and Tomko 1971). Being depended on bridge deck section shape and as a function of reduced wind speeds, the flutter derivatives can be applied to a full bridge as to evaluate bridge flutter instability. Wind tunnel tests and numerical calculations based on the CFD are often employed to identify the flutter derivatives of bridge decks. The CFD calculation for the flutter derivatives is a new and progressive approach that is increasing in strength and sophistication with better visualization and flexibility. Although CFD simulation is still under

---

∗Corresponding author, Professor, E-mail: minggu@tongji.edu.cn

[a] Professor, email: zwzhu@hnu.edu.cn

development, it will become more powerful with the improvement of computer resource and CFD software, especially in bridge early design stage.

Up to now, many researchers devoted their efforts on CFD calculations to predict the flutter derivatives. According to currently available reports, the methods can be categorized into two groups based on imposed vibration mode of bridge deck in CFD simulations. The first one is the imposed harmonic excitation of bridge decks with various schemes. Larsen and Walther (1997) developed a grid-free discrete vortex method which is applicable to bridge decks to extract flutter derivatives. Other reports include the finite difference method (FDM) (Jeong and Kwon 2003, Zhu *et al.* 2009), the finite volume method (FVM) (Vairo 2003, Shirai *et al.* 2003, Zhu *et al.* 2007, Starossek and Aslan 2009) and the finite element method (FEM) (Frandsen 2004, Ge and Xiang 2008). In this group, separate CFD simulations in vertical and torsional vibration under each reduced wind speed are required to calculate the eight flutter derivatives of bridge decks based on system identification (Scanlan and Tomko 1971).

Although the first group using the harmonic vibration is very straightforward, this method has to carry out repeat simulations under each reduced wind speed, which may be time-consuming and not as efficient as the second group. In the second group, forced vibration of bridge decks is still used in CFD, but the vibration mode is no longer unique-frequency motion, but changes to multi-frequency or band-ranged frequency motion. Brar *et al.* (1996) made the first attempt to apply the indicial approach by using the FEM-based CFD calculations, so as to numerically compute the indicial aerodynamic forces exerting on a thin airfoil and a rectangular bluff-body section. Flutter derivatives were obtained through the Fourier transform with the indicial functions. Compared with the method using the imposed harmonic motion on bridge decks, the indicial approach saves significant CPU time since only one simulation is needed to evaluate the transfer function in heaving or pitching motion, when dealing with the whole range of reduced wind speed of interest. However, the study assumed a uniform velocity field in space at the initial time to simulate the step-wise motion, which did not respect the real physics of transient flow. Fransos and Bruno (2006) extended the method with a smoothed-ramp motion to numerically calculate the aerodynamic transfer functions. The flutter derivatives can be simply obtained by evaluating the ratio between the Fourier transforms of output and input, provided that the inverse of the latter is not singular. They further extended the method to investigate Reynolds number effects on flutter derivatives of a flat plate (Bruno and Fransos 2008), and studied the characterization of the aerodynamic and aeroelastic behavior of a flat plate under uncertain flow conditions (Bruno *et al.* 2009). Huang (2011) presented an imposed multi-frequency vibration mode, which is a direct extension of the method in the first group.

This paper presents a method to identify flutter derivatives of bridges based on CFD calculations, system identification and system simulation. The present method employs a smooth exponential function as the imposed motion on bridge decks in CFD. The time histories of aerodynamic forces acting on the bridge deck can be calculated. Then the ARMA model will be used as a function to relate the imposed motion and the aerodynamic time histories. This will allow one to establish a discrete-time aerodynamic model of the bridge deck. The aerodynamic model will be used to simulate output of the aerodynamic forces to an input of harmonic vibration. Then flutter derivatives of bridge decks can be identified by using the Scanlan's model. This method has been applied to a hexagon thin plate and a real bridge deck, and the identified flutter derivatives are compared with the Theodorsen closed-form solution and those from wind tunnel tests.
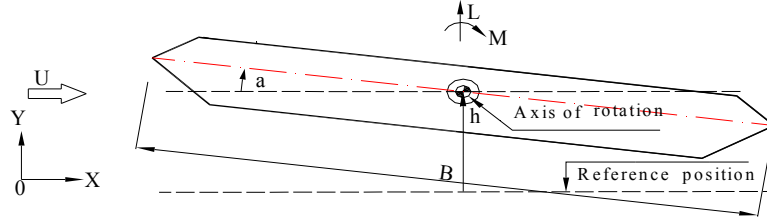
Fig. 1 Bridge deck in smooth flow with two degrees of freedom

2. Governing equations and CFD procedures

Consider a bridge deck enveloping in smooth flow and oscillating with two degrees of freedom, as shown in Fig. 1. Through applying ALE formulations to the rigid body with oscillating boundaries, the equations governing the two-dimensional incompressible flow around the bridge deck can be expressed as follows (Nomura 1992)

$$\frac{\partial u}{\partial x} + \frac{\partial u}{\partial y} = 0$$
(1a)

$$\frac{\partial u}{\partial t} + u_r \frac{\partial u}{\partial x} + v_r \frac{\partial u}{\partial y} + \frac{1}{\rho} \frac{\partial p}{\partial x} = \frac{\mu}{\rho} (\frac{\partial^2 u}{\partial x^2} + \frac{\partial^2 u}{\partial y^2}) - \omega v$$
(1b)

$$\frac{\partial v}{\partial t} + u_r \frac{\partial v}{\partial x} + v_r \frac{\partial v}{\partial y} + \frac{1}{\rho} \frac{\partial p}{\partial x} = \frac{\mu}{\rho} (\frac{\partial^2 v}{\partial x^2} + \frac{\partial^2 v}{\partial y^2}) + \omega u$$
(1c)

where x and y are the along-wind and cross-wind coordinates in a fixed reference frame, respectively; u and v denote the absolute velocities in x and y directions, respectively; t is the time; p the static pressure; μ the molecular viscosity; ω the circular frequency of a moving reference frame in the fixed reference frame; u_r and v_r the fluid velocities relative to the moving reference frame, respectively. In Eq. (1), no turbulence models have been adopted, since the present study involves low Reynolds number flow, as indicated in Subsection 7.1 and 7.2.

In numerical calculations, Eq. (1) is firstly transformed into a conservation form as to be adopted by the FVM. In order to facilitate the incompressible computation, a second-order Projection scheme (Zhu *et al*. 2009) is employed as to decouple the pressure and velocity fields. In the first step, estimation on the velocity field is obtained based on the modified momentum equation. It follows that the pressure field is evaluated through solving the Poisson-type equation with the obtained velocity estimation. In the third step, with the obtained pressure field the estimated velocity is updated in order to get an improved estimation.

The decoupled equations are then discretized in space on the staggered grids, with velocity variables defined on cell edges and pressure variables defined in cell center. For spatial discretization of the equations, a second-order upwind scheme for the convective terms is used, with a second-order central-difference scheme for both the diffusive terms and pressure terms, while advancement in time is accomplished by the second-order implicit Euler scheme. The

resultant difference equations are then solved by the Tri-Diagonal Matrix Algorithm. A multi-grid strategy is employed in order to improve the iterative convergence of the pressure equation. A self-developed code based on the Fortran Language is used to perform CFD simulations. More details can be found in the reference (Zhu *et al*. 2007).

3. Imposed motion on bridge decks

From the system point of view, the fluid field around the bridge deck can be treated as a system. In order to get the system's information, system identification technique may be applied. Commonly, the system's inherent features can be recovered based on the system's input and output information, where the system's output is the response of the system to the input. However, in order to accurately identify the system, suitable input is required as to fully excite the system and get the desired response. For the aerodynamic system of bridge decks, suitable imposed motion on the bridge deck as input which can excite the desired system response would be preferable. Such kind of imposed motion can be as a step-wise displacement or angle change, or as the white-noise time series. However, step-wise changes of displacement will result in computational difficulties in CFD, in which its derivatives versus time correspond to an infinite velocity. Modified step change during a limited time will always involve non-physical oscillations (Zhu *et al*. 2007), even with numerical divergence because of the large and sudden velocity change. For the white-noise time series as the imposed motion, it will be very expensive since a huge amount of time steps have to compute as to effectively identify the system.

For flutter prediction of a real bridge, normally the flutter derivatives will be required under a range of reduced wind speeds of interest. One can choose the input time series with its main energy distributed over a frequency range of interest. The smooth-wise exponential function (Fransos and Bruno 2006), which can be easily implemented in CFD and as shown in Eq. (2), is adopted and discretized into time series, and used as the imposed motion of the bridge deck in the CFD.

$$V(t) = d_0 e^{-w(t-t_0)^2}$$
(2)

The corresponding velocity can also be discretized into time series, and are imposed to the rigid bridge section as the boundary conditions in CFD:

$$\dot{V}(t) = -2w(t-t_0)d_0 e^{-w(t-t_0)^2}$$

$$= -2w(t-t_0)V(t)$$
(3)

where d_0 is the amplitude, corresponding to the maximum displacement imposed on the bridge section, which should be always limited in order to satisfy the linear assumption of small disturbance; t_0 is the moment when $V(t)$ reaching the peak; w denotes the effective width of the exponential function, representing the energy distribution in the frequency domain.

Fig. 2 plots three exponential time series with the same amplitude d_0/B in heaving motion and different value of w; Fig. 3 shows their energy distribution over the reduced frequency axis by means of power spectrum analysis. From the figure, one can see that their dominant energy is concentrated on a limited range of frequency, and a small value of w corresponds to a narrow

shoulder. It should be pointed out that, in order to avoid any computational difficulty, such as numerical oscillation and divergence, a symmetric exponential time series with the beginning and ending data almost close to zero should be employed. Thus a small value of *w* means a long time series. For bridge flutter analysis, flutter derivatives are often required under a range of the reduced wind speed *U/fB*, such as 2~12. Since *U* and *B* are always prescribed in CFD, a range of frequency means a range of reduced wind speeds, with the low frequency corresponding to the high value of reduced wind speed. Based on the consideration of CPU time and the desired reduced wind speed, the exponential function with value *w* of 150 will be used in the following study.
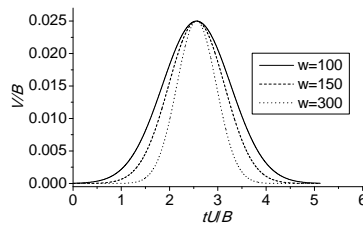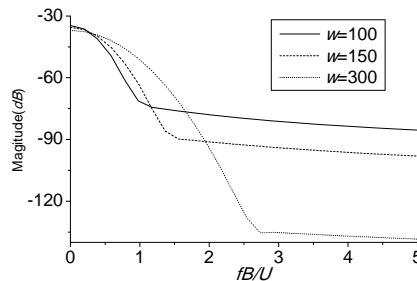

Fig. 2 Exponential function with different *w*

Fig. 3 Power spectrum analysis of time series

4. Establish aerodynamic models of the bridge deck

When the bridge deck is forced to undergo an imposed heaving or pitching motion, the aerodynamic forces acting on the bridge deck can be evaluated from the CFD. In this paper, the interval for both the imposed motion and the collecting aerodynamic forces uses the same time step size. Treating the imposed motion of the bridge deck as the input and the computed aerodynamic forces as the outputs, the relationship between the input and output can be established based on system identification techniques. Such kind of relationship between the input and output is the inherent characteristic of bridge aerodynamics, and can be obtained by system identification.

In this paper, the Auto-Regressive Moving Average (ARMA) model (Brockwell and Davis 2009) is employed to establish a relationship between the imposed motion and the aerodynamic forces. In the following, this kind of established relationship is referred to as 'aerodynamic models'.

It should be stressed that the aerodynamic forces from the CFD solution include both the lift and moment either for the heaving or pitching motion. The unique-input double-output ARMA model should be employed straightforwardly to train the input-output relationship. However, using unique-input double-output ARMA models will complicate the identification and will be time-consuming. Therefore, this paper employs the unique-input unique-output ARMA model to simplify the identification. Four ARMA models are applied herein: a lift model for the lift induced by the heaving motion (hereafter referred to as lift-heaving model); a moment model for the moment induced by the heaving motion (hereafter referred to as moment-heaving); a lift model for the lift induced by pitching motion (hereafter referred to as lift-pitching) and a moment model for the moment induced by pitching motion (hereafter referred to as moment-pitching). The present results indicate that the unique-input unique-output ARMA model is suitable for identification of flutter derivatives of bridge decks.

The relationships between the aerodynamic forces and the imposed motion in the four models can be assumed to satisfy the following discrete-time ARMA model

$$y(t) = \sum_{i=1}^{na} a_i y(t-i) + \sum_{j=0}^{nb} b_j V(t-j) \qquad (4)$$

where $y(t)$ is the output (the aerodynamic force); $V(t)$ is the input (the imposed motion); a_i and b_j are the scale coefficients corresponding to the input and output terms, respectively; na and nb are the orders of the respective polynomials. Eq. (4) indicates that the aerodynamic output at time t is the sum of the weighted aerodynamic outputs and the weighted displacement inputs at present and past time steps.

The aerodynamic forces acting on the bridge deck may contain a steady value, such as the steady static lift and moment before the forced displacement imposed. While Eq. (4) does not include any constant terms as to account for the steady state in output. Hence, before system identification an additional step is necessary to remove the static forces from the computed force time histories. In the following, the aerodynamic time series with the steady value removed will still be called the aerodynamic forces. Herein, the data from the CFD, including the time step size, the imposed bridge deck motion and the computed aerodynamic forces, will be called as "Training data", and one can use them to train the input-output relationship based on the ARMA model, and finally obtain the bridge deck aerodynamic models.

In Eq. (4), two groups of parameters, i.e., the orders of the respective polynomials and the corresponding scale coefficients, should be determined. A feasible step is firstly assuming the input and output orders, and then fitting the corresponding input and output coefficients. With the training data, these input and output model coefficients can be fitted straightforward by using the least square algorithm. This can be done on the software platform of MATLAB. Then one can transfer to other combination of the input and output orders, and fit their input and output coefficients.

For various ARMA models with different input and output orders, attempt should be made to find an accurate one, since they may present different predictions even to the same input. In order to choose an ARMA model which can give a more accurate prediction, comparisons of the output

between different ARMA models to the same input should be carried out. One can define a parameter reflecting the discrepancy between the computed aerodynamic forces from CFD and those simulated by the ARMA model, where the imposed sectional motion is used as the input in this study. Bear in mind that the same time step size as in the CFD should be adopted. The defined parameter can take the following form

$$\sigma = \sqrt{\frac{\sum_{i=1}^{n}(y_i - \hat{y}_i)^2}{n}}$$ (5)

where n is the number of the training data; y_i is the aerodynamic force from the CFD when the bridge deck undergoing the imposed motion; $\hat{y}_i$ is the aerodynamic force simulated by the ARMA model to the same imposed motion.

In this paper, the lift-heaving model will be chosen as an example. The input and output orders are set in the range from first to 30th order and from zero to 30th order, respectively. If the input order is first chosen, such as the 2nd, then successively choosing different output order is performed. With the matched input and output orders, one can fit the model's input and output coefficients, and use this established model to carry out model simulation with the same imposed motion. Then the discrepancy of this ARMA model between the CFD calculation and model simulated can be obtained from Eq. (5). After testing all the input and output orders in the prescribed range, one can compare the discrepancy of different ARMA models with different input and output orders, and find the one with the minimum value of σ. This ARMA model can be regarded as the desired discrete-time lift-heaving model, and will be used to predict the lift induced by bridge deck heaving motion.

5. Model simulations to the simple-harmonic motion

After establishing the discrete-time aerodynamic models of the bridge deck, one can carry out model simulations to any inputs, provided that the frequency contents of the motion can match the frequency feature of the established model. In the following, the sinusoidal function is discretized into time series and used as model input in heaving and pitching motion

$$X = X_0 \sin(2\pi f t)$$ (6)

where X_0 is the amplitude, i.e., vertical maximum for heaving or torsional maximum for pitching, which is equal to d_0 in Eq. (3); f the frequency and can be set up as to get the reduced wind speeds based on U/fB. Since U and B are already prescribed in CFD, varying the frequency can result in different reduced wind speeds. Hence in model simulations, the frequency of the simple-harmonic time series can be calculated based on the desired reduced wind speed with the known value of U/B=10. This strategy will be consistent with the CFD if the same time step size is used in the model simulation. Because the established aerodynamic models represent the aerodynamic inherent features of the bridge deck over the frequency of interest, certainly the aerodynamic models can simulate aerodynamic forces to a suitable displacement inputs. The same time step size as that in CFD is used for model simulations, because the CPU time required for

model simulations is significantly smaller than that in CFD. In order to extract flutter derivatives under a couple of desire reduced wind speeds, a couple of individual model simulations should be performed, in which a different frequency in Eq. (6) will be used.

6. Identification of flutter derivatives

The self-excited aeroelastic forces acting on the bridge deck are commonly expressed in the following form (Scanlan and Tomko 1971),

$$L = \frac{1}{2}\rho U^2 B\left(KH_1^* \frac{\dot{h}}{U} + KH_2^* \frac{B\dot{\alpha}}{U} + K^2 H_3^* \alpha + K^2 H_4^* \frac{h}{B}\right) \tag{7a}$$

$$M = \frac{1}{2}\rho U^2 B^2\left(KA_1^* \frac{\dot{h}}{U} + KA_2^* \frac{B\dot{\alpha}}{U} + K^2 A_3^* \alpha + K^2 A_4^* \frac{h}{B}\right) \tag{7b}$$

where K is defined as $\omega B / U$ and is known as the reduced frequency, in which ω denotes the circular frequency; H_i^* and $A_i^* (i=1,2,3,4)$ are the flutter derivatives. Eq. (7) indicates that, with the input of simple-harmonic motion and its first derivatives (velocity), as well as the simulated time histories of aerodynamic forces, the flutter derivatives can be identified using a system identification technique. In this paper, the least square algorithm is employed.

Considering the pure heaving motion, Eq. (7) can be simplified as follows

$$L = \frac{1}{2}\rho U^2 \cdot B \cdot \left(KH_1^* \frac{\dot{h}}{U} + K^2 H_4^* \frac{h}{B}\right) \tag{8a}$$

$$M = \frac{1}{2}\rho U^2 \cdot B^2 \cdot \left(KA_1^* \frac{\dot{h}}{U} + K^2 A_4^* \frac{h}{B}\right) \tag{8b}$$

where the heaving displacement and velocity at a certain time step i are marked as h_i and $\dot{h}_i$, respectively; the lift and moment at time step i are denoted by L_i and M_i, respectively.

Eq. (8) can be rewritten in the following matrix form

$$\begin{Bmatrix} L_i \\ M_i \end{Bmatrix} = \begin{bmatrix} \frac{1}{2}\rho UBK\dot{h}_i & \frac{1}{2}\rho U^2 K^2 h_i & & \\ & & \frac{1}{2}\rho UB^2 K\dot{h}_i & \frac{1}{2}\rho U^2 BK^2 h_i \end{bmatrix} \tag{9}$$

Let

$$\{X\} = \begin{Bmatrix} H_1^* & H_4^* & A_1^* & A_4^* \end{Bmatrix}^T \tag{10}$$

$$\{F_i\} = \begin{Bmatrix} L_i & M_i \end{Bmatrix}^T \tag{11}$$

and

$$[C_i] = \begin{bmatrix} \frac{1}{2}\rho UBK\dot{h}_i & \frac{1}{2}\rho U^2 K^2 h_i & & \\ & & \frac{1}{2}\rho UB^2 K\dot{h}_i & \frac{1}{2}\rho U^2 BK^2 h_i \end{bmatrix} \tag{12}$$

then, Eq. (9) can be rewritten as

$$\{F_i\} = [C_i]\{X\} \tag{13}$$

Eq. (13) with total *n* time-step data can be formulated as

$$\begin{Bmatrix} F_1 \\ \vdots \\ F_i \\ \vdots \\ F_n \end{Bmatrix} = \begin{bmatrix} C_1 \\ \vdots \\ C_i \\ \vdots \\ C_n \end{bmatrix} \{X\} \tag{14}$$

Eq. (14) can not be solved exactly if $n \succ 2$ because it is over-determined. However, it can be evaluated by using the least square method, which produces an estimation of the flutter derivatives as follows

$$\{X\} = \left(\begin{bmatrix} C_1 \\ \vdots \\ C_i \\ \vdots \\ C_n \end{bmatrix}^T \begin{bmatrix} C_1 \\ \vdots \\ C_i \\ \vdots \\ C_n \end{bmatrix} \right)^{-1} \begin{bmatrix} C_1 \\ \vdots \\ C_i \\ \vdots \\ C_n \end{bmatrix}^T \begin{Bmatrix} F_1 \\ \vdots \\ F_i \\ \vdots \\ F_n \end{Bmatrix} \tag{15}$$

A similar way can be used to recover the flutter derivatives relating to the pitching motion.

7. Applications and results

7.1 Identification of flutter derivatives of a hexagon thin plate

To validate the present approach for identification of flutter derivatives, a hexagon thin plate model is taken as a case study. This plate section has a width of 450 mm and height of 20 mm, with sharp corners at windward and leeward side. It was used as a model in wind tunnel

experiments (Gu *et al*. 2000, Gu and Qin 2004), as shown in Fig. 4.

Fig. 5 shows the computational domain and grids around the hexagon thin plate. The computational domain is a rectangle, with inlet, outlet and side boundaries being 15*B* (*B* the plate width) away from the plate. The total grids number is 130×98, non-uniform structured meshes are employed in order to reflect the variable gradients in the computational domain. The grids near the surface of the plate are highly stretched, with the first grid space of 0.005*B* normal to the wall. Additionally, a multi-grid algorithm based on "V" cycle iteration, with three layers of grid system and every second fine grid being the coarse one, is employed as to improve the iterative convergence when solving the pressure equation (Zhu *et al*. 2009). During the CFD calculation, the exponential time series are imposed to the hexagon thin plate when undergoing heaving or pitching motion. The value of d_0 for heaving or pitching motion is 0.025*B* and 3°, respectively. The Reynolds number is of 300, and the computational time step size is 0.0005s.

With the present ALE formulation, the grid system is fixed with the rigid section and moving synchronously according to the imposed motion. At each time step, the no-slip and no-penetration conditions are applied to the surface of the thin plat. At each time step, velocity of the moving reference frame can be projected onto the grids system, with the incoming wind speed onto the inlet, the top and bottom boundaries. For the Projection-2 scheme on staggered grids, the Neumann boundary condition for pressure is applied on the outlet boundary.

The lift and moment coefficients are respectively defined as follows

$$C_L = L/(1/2\rho U^2 B) \tag{16a}$$

$$C_M = M/(1/2\rho U^2 B^2) \tag{16b}$$

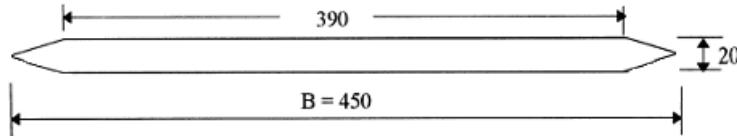Fig. 4 Cross section of hexagon thin plate (unit: mm)

(a)   (b)
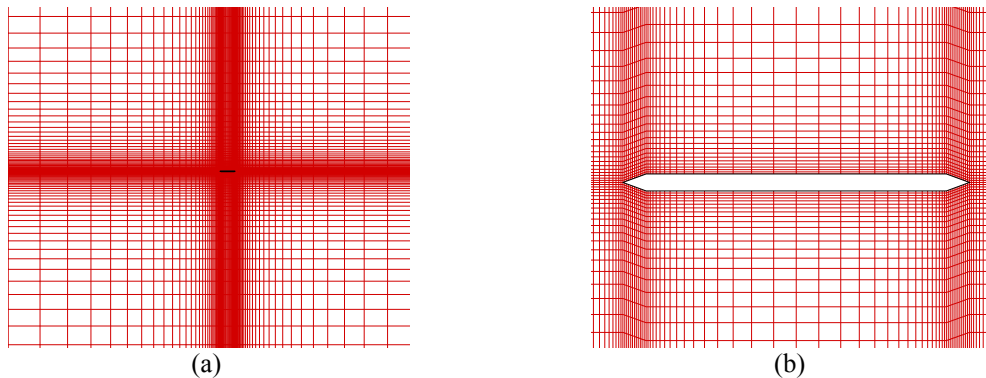
Fig. 5 Computational domain and grids around hexagon thin plate (a) Computational domain and grids and (b) Close-up view
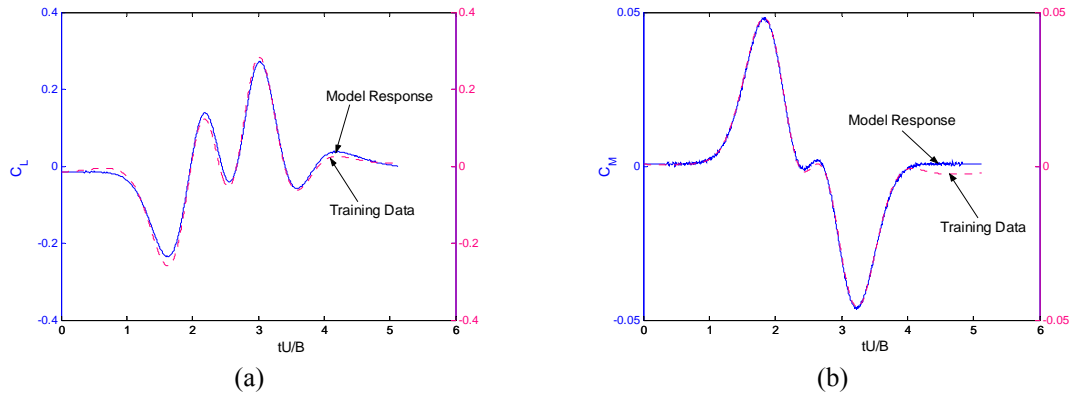
Fig. 6 Comparison of aerodynamic coefficients between model simulation and training data in heaving motion (a) Lift coefficient and (b) Moment coefficient
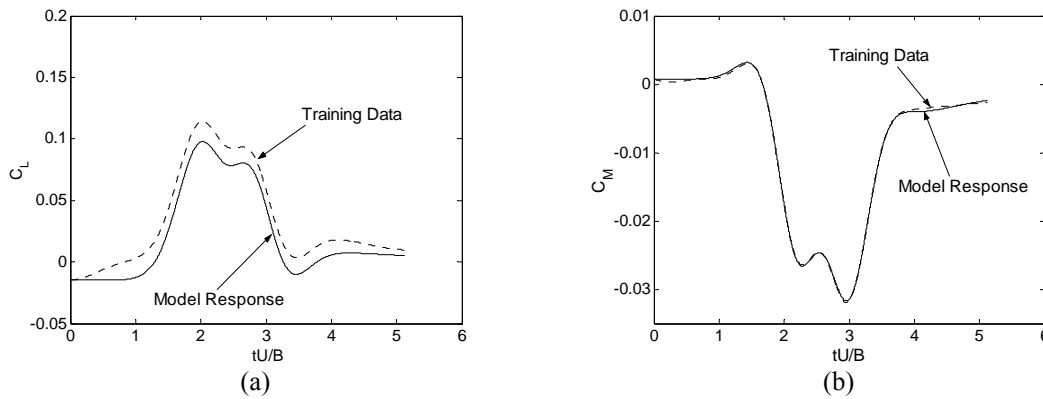

Fig. 7 Comparison of aerodynamic coefficients between model simulation and training data in pitching motion (a) Lift coefficient and (b) Moment coefficient

When the hexagon thin plate is forced to undergo imposed heaving or pitching motion, the aerodynamic forces acting on the plate can be calculated. Their coefficients are plotted by dash lines and labeled (Training Data) in Figs. 6 and 7.

The training data of the system includes the computed aerodynamic forces and the imposed motion at each time step. With the training data and system identification technique applied to the ARMA model, one can obtain four discrete-time aerodynamic models, with more accurate predictions on the aerodynamic forces: the lift-heaving model with 22nd-order input and first-order output; the moment-heaving model with only 22nd-order input; and 12th-order inputs and first-order output for both the lift-pitching and moment-pitching models. The solid lines in Figs. 6 and 7 (labeled as Model Response) show the aerodynamic forces simulated by these four models to the imposed motion in CFD. It is evident that all of the model responses and their training data have the same trends. Except for the response produced by the lift-pitching model, the model responses

match the training data fairly well.

Different model orders have been tried to fit the input and the output when dealing with the lift-pitching model, in order to improve the discrepancy between the simulated time series and the training data. It is found that decreasing the order of input and output will enlarge the discrepancy, while to some extent, increasing the order will not apparently improve the situation. Further increasing the order may result in high-frequency numerical oscillation around the training data, and may even result in divergence. Considering the computational efficiency, lower order models will be adopted when different models present almost the same accuracy.

In order to predict the aerodynamic force (i.e., the outputs) of the models to a simple-harmonic displacement input, model simulations are carried out with the sine function. Value of X_0 is $0.025B$ for heaving and 3° for pitching. The time step size is 0.0005s. Fig. 8 plots time histories of the simulated lift coefficients of the lift-heaving model, as well as the moment coefficients of the moment-heaving model, both to a simple-harmonic heaving motion with a frequency of 2 *Hz* (see Fig. 9). One can see that both of the simulated time histories appear in a simple-harmonic mode, with phase lags included between the input and output.
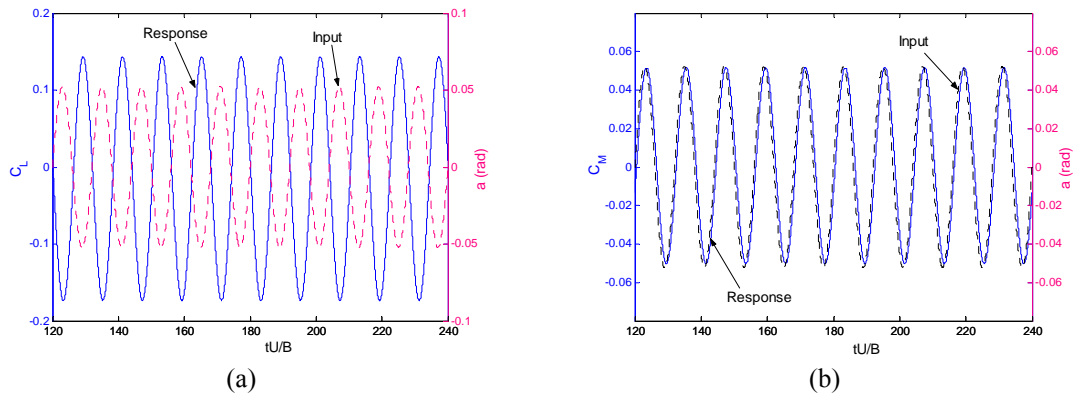

Fig. 8 Time histories of force coefficients simulated by aerodynamic models of hexagon thin plate in heaving motion (a) Input and Lift coefficient, (b) Input and Moment coefficient
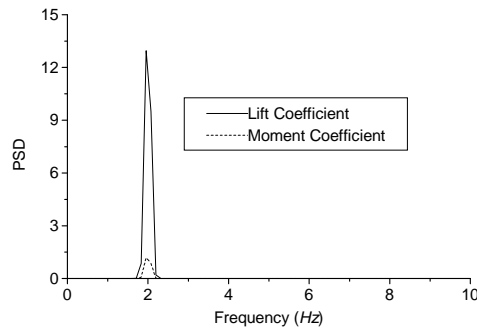

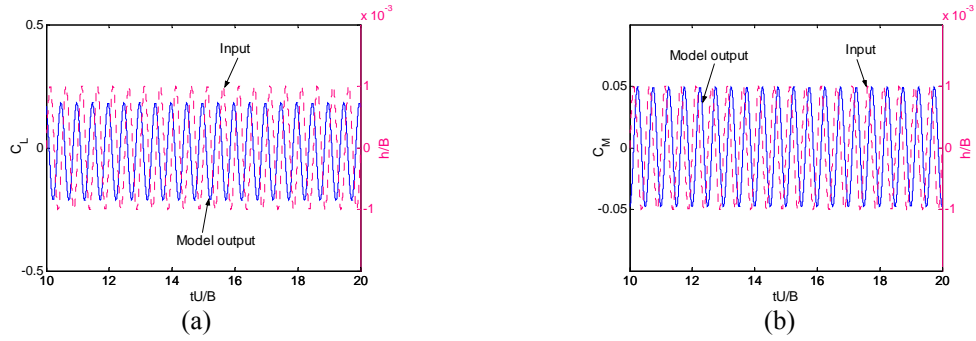Fig. 9 PSD analysis of simulated lift and moment coefficients

Fig.10 Time histories of force coefficients simulated by aerodynamic models of hexagon thin plate in pitching motion (a) Input and Lift coefficient, (b) Input and Moment coefficient
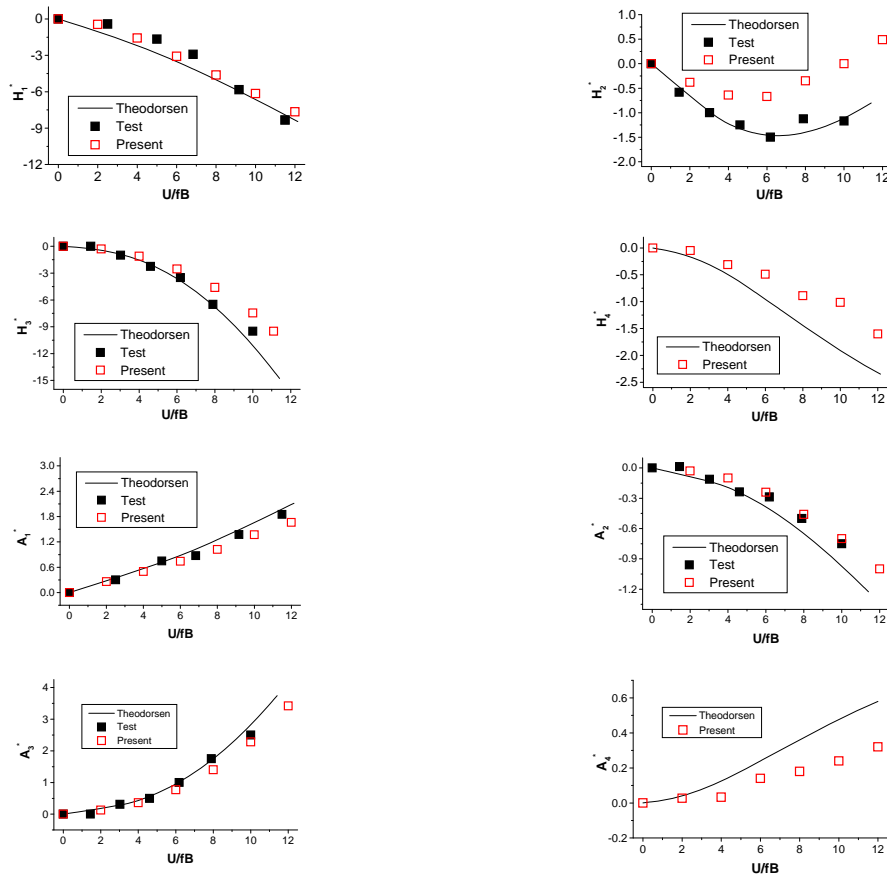

Fig. 11 Identified flutter derivatives of hexagon thin plate in comparison with Theodorsen closed-form solution and results from wind tunnel test

Fig. 10 shows the simulated time histories of the lift coefficients from the lift-pitching model, as well as the moment coefficients from the moment-pitching model, both to the simple-harmonic pitching motion with a frequency of 5 *Hz*.

With the time histories of both input and output, the flutter derivatives at a given reduced wind speed can be identified. In order to extract the flutter derivatives at a different reduced wind speed, procedures include changing the frequency of the input, repeating the model simulation steps and performing system identification. The identified flutter derivatives H_i^* and A_i^* (i=1, 2, 3, 4) at various reduced wind speeds, together with the Theodorsen closed-form solution (Theodorsen, 1936) and the results from the wind tunnel (Gu *et al*. 2000), are plotted in Fig. 11. The wind tunnel test (Gu *et al*. 2000) was carried out in smooth flow with the Reynolds number ranging from 1.3×10^5 to 7.2×10^5. One can see that the present results share common trends with the closed-form solution and those from wind tunnel tests. Except for H_2^*, the identified flutter derivatives are close to results from the wind tunnel.

It should be pointed out that the employed governing equations for fluid do not include the turbulent model, while the present Reynolds number is much lower than that in wind tunnel. It seems that the flutter derivatives of sharp corner sections may be insensitive to Reynolds number and turbulence (Frandsen 2004).

7.2 Identification of flutter derivatives of a real bridge deck

The present approach is applied to the Humen Bridge. This bridge is located in the southern part of China crossing the Zhujiang River, which is one of the most active typhoon-prone regions in the world. Flutter stability evaluation is of first importance when designing long-span bridges in such areas. This is a single-span two-hinge suspension bridge with the central span of 888 m. Its stiffening girder is a streamlined box girder of 35.6 m width and 3.012 m height, as shown in Fig. 12.

Fig.13 shows the computational grids around the bridge deck. The computational domain and grids, initial and boundary conditions, as well as the Reynolds number and the imposed motion are almost the same as those used in the hexagon thin plate, except that the first grid space is of 0.004*B* normal to the wall. The computational time step size is of 0.0004s.

The aerodynamic forces acting on the bridge deck undergoing imposed motion are calculated, as given in Figs. 14 and 15, where the dashed lines are labeled (Training Data). Based on the training data, the employed system identification technique and model screening method, four aerodynamic models are established: the lift-heaving model with 12nd-order input and zero-order output; the moment-heaving model with 10nd-order input and 10nd-order output; 12nd-order input and first-order output for both the lift-pitching and the moment-pitching models. Figs. 14 and 15 show the simulated aerodynamic coefficients, which are labeled as Model Responses of the four models to the imposed motion in CFD. Clearly, all the model responses and training data have the same trends. In particular, the force coefficients simulated by the lift-pitching and moment-pitching models closely match the training data. As for the lift-heaving model, the simulated time histories show slight oscillation around the training data. This may be attributed to fact that the model includes a higher order of input but without any previous output.
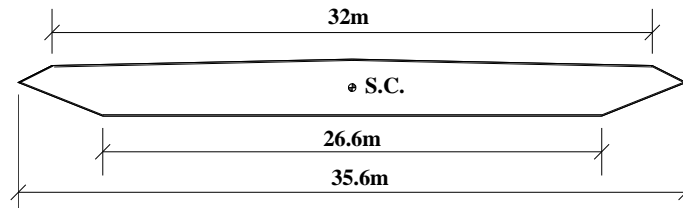
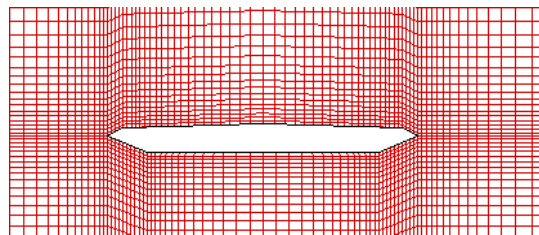Fig. 12 Girder cross section of Humen Bridge

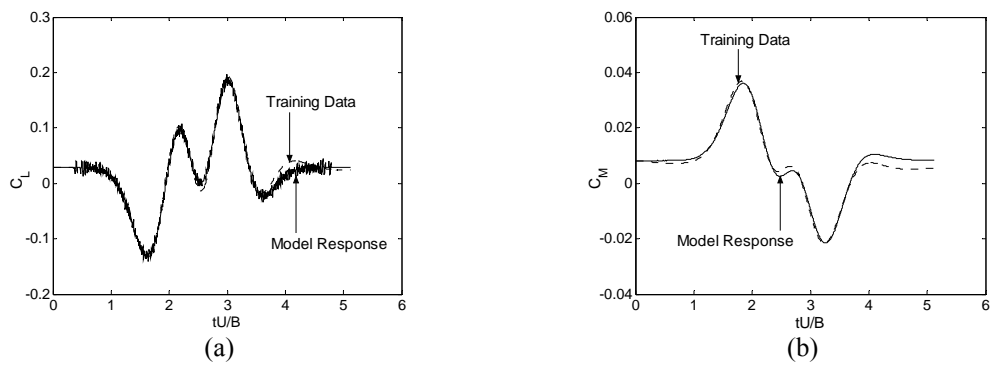Fig. 13 Computational grids around bridge deck

Fig. 14 Comparison of aerodynamic coefficients between model simulation and training data in heaving motion (a) Lift coefficient and (b) Moment coefficient
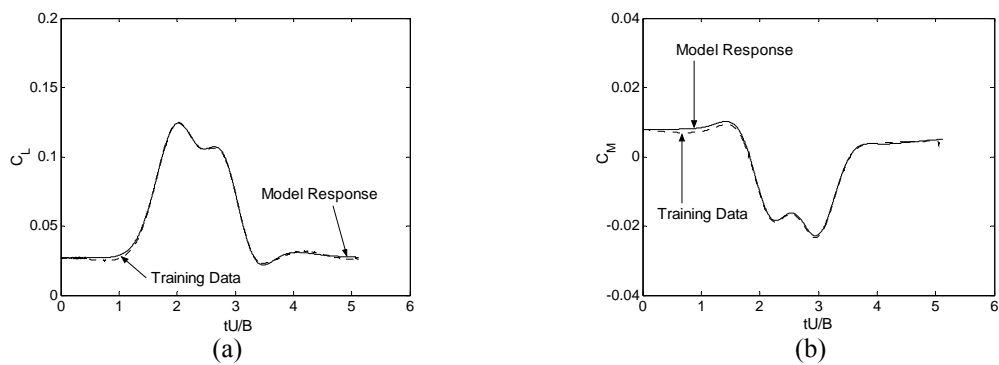
Fig. 15 Comparison of aerodynamic coefficients between model simulation and training data in pitching motion (a) Lift coefficient and (b) Moment coefficient

Fig. 16 shows the simulated lift coefficients of the lift-heaving model, as well as the moment coefficients of the moment-pitching model, both to a simple-harmonic heaving motion with a frequency of 5*Hz* and amplitude of 0.025*B*. Fig. 17 shows the lift coefficients from the lift-pitching model, as well as the moment coefficients from the moment-pitching model, both to a simple-harmonic pitching motion, with frequency of 5*Hz* and pitching amplitude of 3°. Like the situation in the hexagon thin plate, all of the simulated time histories appear in simple-harmonic mode.

The identified flutter derivatives of the bridge deck are plotted in Fig. 18. The direct derivatives, i.e., H_1^*, A_2^* and A_3^*, from the sectional model wind tunnel test (Lin 1995) are also presented in the figure. The wind tunnel test was performed in smooth flow, and its Reynolds number ranges from 1.5×10^5 to 4.9×10^5. It can be seen that the present results match the results from the wind tunnel.

It can be observed again that the identified the flutter derivatives of bridge box girders seem to be insensitive to the Reynolds number and turbulence.
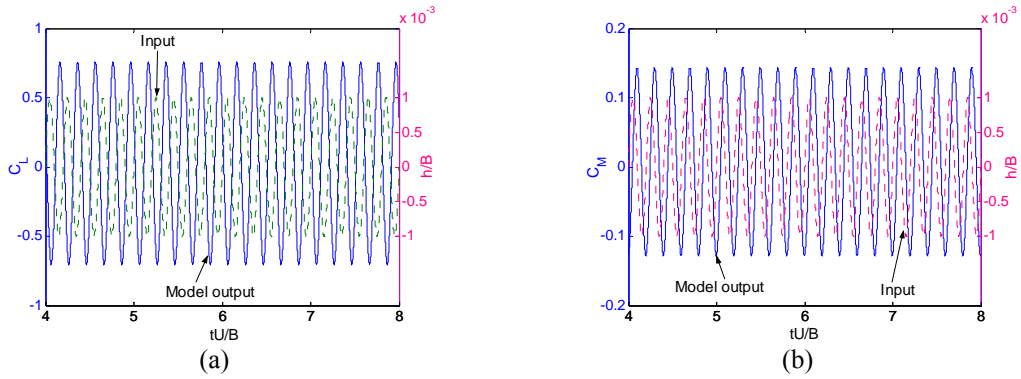

Fig. 16 Time histories of force coefficients simulated by aerodynamic models of bridge deck in heaving motion (a) Input and Lift coefficient and (b) Input and Moment coefficient
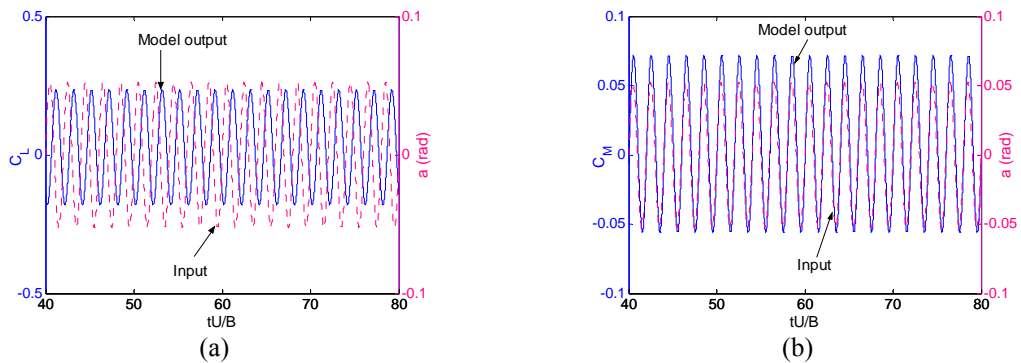

Fig. 17 Time histories of force coefficients simulated by aerodynamic models of bridge deck in pitching motion (a) Input and Lift coefficient and (b) Input and Moment coefficient
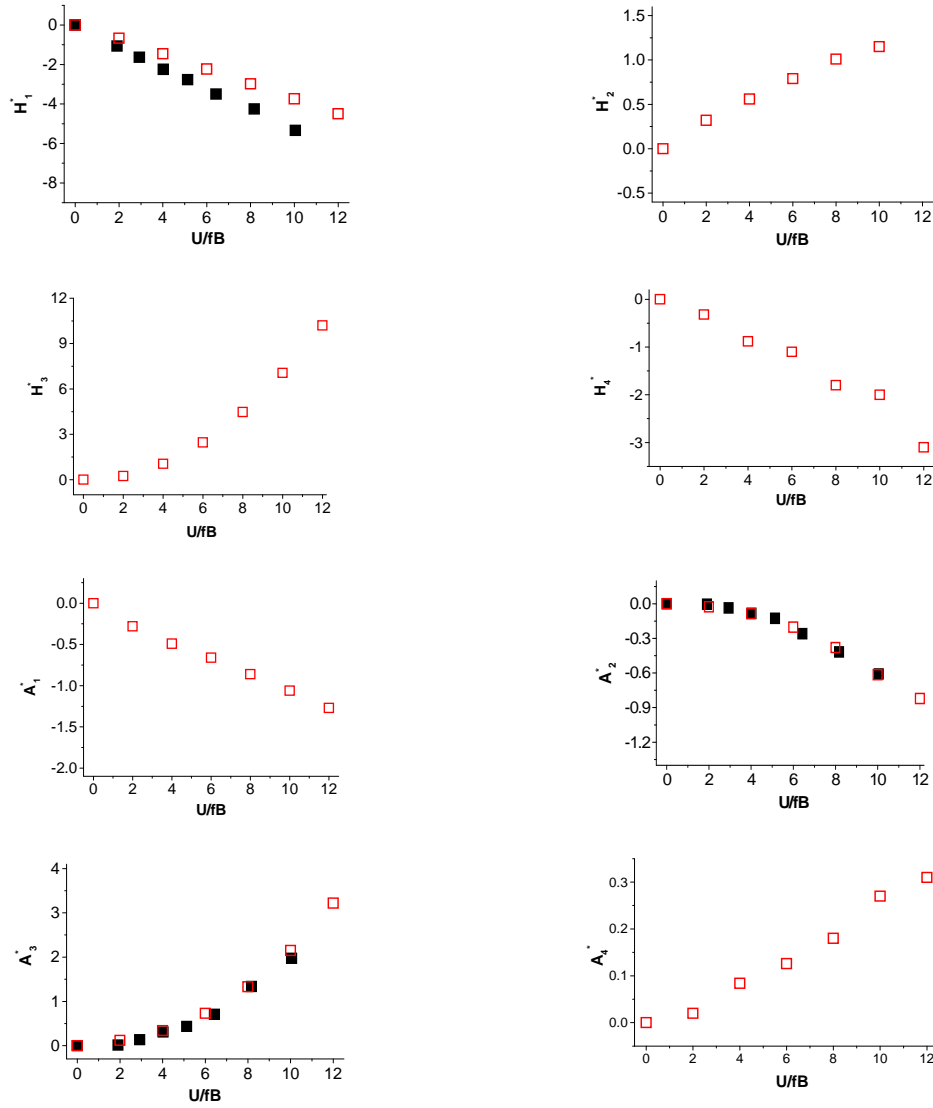
Fig. 18 Flutter derivatives of Humen Bridge deck, (□) flutter derivatives identified by the present method, (■) flutter derivatives identified through wind tunnel tests

8. Conclusions

In this paper, an approach by means of the CFD and the system identification is presented as to establish the discrete-time aerodynamic model, which can be used to identify the flutter derivatives of bridge decks based on the system simulation. The main conclusions and discussions can be summarized as follows,

(1) Compared with the CFD using the imposed simple-harmonic motion to the bridge deck, the present method requires only one CFD calculation in heaving or pitching motion, resulting in

notable time saving in identification of flutter derivatives.

(2) The exponential function (Fransos and Bruno, 2006) is adopted as the impose motion in CFD, in which the frequency contents are adjustable through varying the parameter *w*. The advantage of this function over the unit-step function is that, it is very easy to be implemented in CFD without any numerical difficulties.

(3) Turbulent models are not included in this study, while the Reynolds numbers are near three orders lower than those in wind tunnel. However the identified flutter derivatives of the two sections are in good agreement with the results from wind tunnel. It seems that the flutter derivatives of sharp corner sections are not sensitive to both the Reynolds number and turbulence.

(4) The present method is only validated for streamlined-box sections. Further studies are required as to identify flutter derivatives of bridges with bluff sections. Except for the ARMA model, it may also be a good practice to establish the aerodynamic model based on other system identification methods.

(5) Although the idea of aerodynamic models is used to identify flutter derivatives of bridge decks based on Scanlan's models. It may be a valuable practice to employ the aerodynamic model to directly predict aeroelastic response of bridges when coupled with the structural system. When structural responses evaluated by the dynamic equations are used as displacements input to the aerodynamic models, aerodynamic forces acting on the bridge deck can be predicted by model simulations. Those aerodynamic forces can be in turn put into in the dynamic equations, and one can perform aeroelastic analysis and solve structural response under wind (Zhu *et al.* 2007). The important point is that the Scanlan's model is no longer required when carrying out aeroelastic analysis for bridges. Furthermore, it may be feasible to predict flutter instability of bridges based on the aerodynamic models. This may be a major advantage when predicting aeroelastic response of nonlinear aerodynamic systems, in which large amplitude structural vibration and massive boundary layer separation occur. This discuss on the subject is, however, beyond the scope of this paper.

Acknowledgements

References

Brar, P.S., Raul, R. and Scanlan, R.H. (1996), "Numerical calculation of flutter derivatives via indicial functions", *J. Fluid. Struct.*, **10**(4), 337-351.

Brockwell, P. J. and Davis, R.A. (2009), *Time series: theory and methods* (2nd Ed.), New York, Springer.

Bruno, L., Canuto, C. and Fransos, D. (2009), "Stochastic aerodynamics and aeroelasticity of a flat plate via generalized Polynomial Chaos", *J. Fluid Struct.*, **25**, 1158-1176.

Bruno, L. and Fransos, D. (2008), "Evaluation of Reynolds number effects on flutter derivatives of a flat plate by means of a computational approach", *J. Fluid. Struct.*, **24**(7), 1058-1076.

Frandsen, J.B. (2004), "Numerical bridge deck studies using finite elements, Part I: flutter", *J. Fluid. Struct.*, **19**(2), 171-191.

Fransos, D. and Bruno, L. (2006), "Determination of the aeroelastic transfer functions for streamlined bodies

by means of a Navier-Stokes solver", *Math. Comput. Model.*, **43**(5-6), 506-529.

Ge, Y.J. and Xiang, H.F. (2008), "Computational models and methods for aerodynamic flutter of long-span bridges", *J. Wind Eng. Ind. Aerod.*, **96**(10-11), 1912-1924.

Gu, M. and Qin, X.R. (2004), "Direct identification of flutter derivatives and aerodynamic admittances of bridge decks", *Eng. Struct.*, **26**(14), 2161-2172.

Gu, M., Zhang, R.X. and Xiang, H.F. (2000), "Identification of flutter derivatives of bridge decks", *J. Wind Eng. Ind. Aerod.*, **84**(2), 151-162.

Huang, L. and Liao, H. (2011), "Identification of flutter derivatives of bridge deck under multi-frequency vibration", *Eng. Appl. Comput. Fluid. Mech.*, **5**(1) , 16-25.

Jeong, U.Y. and Kwon, S.D. (2003), "Sequential numerical procedures for predicting flutter velocity of bridge sections", *J. Wind Eng. Ind. Aerod.*, **91**(1-2), 291-305.

Larsen, A. and Walther, J.H. (1997), "Aeroelastic analysis of bridge girder sections based on discrete vortex simulation", *J. Wind Eng. Ind.Aerod.*, **67-68**, 253-265.

Lin, Z.X. and Xiang, H.F. (1995), *Researches on wind-induced instability of Humen Bridge in erection stage*, Technical Report of State Key Laboratory for Disaster Reduction in Civil Engineering, Tongji University, Shanghai, (in Chinese).

Nomura, T. and Hughes, T.J.R. (1992), "An arbitrary Lagrangian-Eulerian finite element method for interaction of fluid and a rigid body", *Comput. Meth. Appl.*, **95**(1), 115-138.

Scanlan, R.H. and Tomko J.J. (1971), "Airfoil and bridge deck flutter derivatives", *J. Eng. Mech. - ASCE*, **97**(6), 1171-1737.

Shirai, S. and Ueda, T. (2003), "Aerodynamic simulation by CFD on flat box girder of super-long-span suspension bridge", J. *Wind Eng. Ind Aerod.*, **91**(1-2), 279-290.

Starossek, U. and Aslan, H. (2009), "Experimental and numerical identification of flutter derivatives for nine bridge deck sections", *Wind Struct.*, **12**(6), 519-540.

Theodorsen, T. (1935), *General theory of aerodynamic instability and the mechanism of flutter*, NACA Report No.496, 413-433.

Vairo, G. (2003), "A numerical model for wind loads simulation on long-span bridges", *Simul. Model. Pract. Th.*, **11**(5-6), 315-351.

Zhu, Z.W., Chen Z.Q. and Gu, M. (2009), "CFD based simulations of flutter characteristics of ideal thin plates with and without central slot", *Wind Struct.*, **12**(1), 1-19.

Zhu, Z.W., Gu, M. and Chen, Z.Q. (2007), "Wind tunnel and CFD study on identification of flutter derivatives of a long-span self-anchored suspension bridge", *Comput. Aided Civil Infrastruct. Eng.*, **22**(8), 541-554.

CC